

# eScholarship@UMassChan

## Nucleic Acid Aptamers Protect Against Lead (Pb(II)) Toxicity [preprint]

Item Type	Preprint
Authors	Anwar, Afreen;De Ayreflor Reyes, Solimar Ramis;John, Aijaz Ahmad;Breiling, Erik;O'Connor, Abigail M;Reis, Stephanie;Shim, Jae-Hyuck;Shah, Ali Asghar;Srinivasan, Jagan;Farny, Natalie G
Citation	Anwar A, De Ayreflor Reyes SR, John AA, Breiling E, O'Connor AM, Reis S, Shim JH, Shah AA, Srinivasan J, Farny NG. Nucleic Acid Aptamers Protect Against Lead (Pb(II)) Toxicity. bioRxiv [Preprint]. 2024 Mar 31:2024.03.28.587288. doi: 10.1101/2024.03.28.587288. PMID: 38585880; PMCID: PMC10996642.
DOI	<a href="https://doi.org/10.1101/2024.03.28.587288">10.1101/2024.03.28.587288</a>
Journal	bioRxiv : the preprint server for biology
Rights	The copyright holder for this preprint is the author/funder, who has granted bioRxiv a license to display the preprint in perpetuity. It is made available under a <a href="https://creativecommons.org/licenses/by-nc-nd/4.0/">CC-BY-NC-ND 4.0 International license</a> .;Attribution-NonCommercial-NoDerivatives 4.0 International
Download date	2025-04-21 15:36:14
Item License	<a href="http://creativecommons.org/licenses/by-nc-nd/4.0/">http://creativecommons.org/licenses/by-nc-nd/4.0/</a>
Link to Item	<a href="https://hdl.handle.net/20.500.14038/53374">https://hdl.handle.net/20.500.14038/53374</a>

1 Nucleic Acid Aptamers Protect Against Lead (Pb(II)) Toxicity

2

3 Afreen Anwar<sup>1,2</sup>, Solimar Ramis De Ayreflor Reyes<sup>1</sup>, Aijaz Ahmad John<sup>3</sup>, Erik Breiling<sup>1</sup>,  
4 Abigail M. O'Connor<sup>1</sup>, Stephanie Reis<sup>1</sup>, Jae-Hyuck Shim<sup>3,4,5</sup>, Ali Asghar Shah<sup>2</sup>, Jagan  
5 Srinivasan<sup>1,6,7</sup>, Natalie G. Farny<sup>1,6,7\*</sup>

6

7 1 Department of Biology and Biotechnology, Worcester Polytechnic Institute, 100  
8 Institute Road, Worcester, MA, 01609, USA

9 2 Department of Biotechnology, Baba Ghulam Shah Badshah University, Rajouri (J&K),  
10 India

11 3 Department of Medicine, University of Massachusetts Chan Medical School,  
12 Worcester, MA, USA

13 4 Horae Gene Therapy Center, University of Massachusetts Chan Medical School,  
14 Worcester, MA, USA

15 5 Li Weibo Institute for Rare Diseases Research, University of Massachusetts Chan  
16 Medical School, Worcester, MA, USA

17 6 Program in Bioinformatics and Computational Biology, Worcester Polytechnic Institute,  
18 100 Institute Road, Worcester, MA, 01609, USA

19 7 Program in Neuroscience, Worcester Polytechnic Institute, 100 Institute Road,  
20 Worcester, MA, 01609, USA

21 \*Correspondence to N.G.F.: [nfarny@wpi.edu](mailto:nfarny@wpi.edu)

22

23 Keywords:

24 Lead, Pb(II), aptamer, reproductive toxicity, neurotoxicity, *C. elegans*, behavior,  
25 osteoblast

26 **ABSTRACT**

27 Lead (Pb(II)) is a pervasive heavy metal toxin with many well-established negative  
28 effects on human health. Lead toxicity arises from cumulative, repeated environmental  
29 exposures. Thus, prophylactic strategies to protect against the bioaccumulation of lead  
30 could reduce lead-associated human pathologies. Here we show that DNA and RNA  
31 aptamers protect *C. elegans* from toxic phenotypes caused by lead. Reproductive  
32 toxicity, as measured by brood size assays, is prevented by co-feeding of animals with  
33 DNA or RNA aptamers. Similarly, lead-induced behavioral anomalies are also  
34 normalized by aptamer feeding. Further, cultured human HEK293 and primary murine  
35 osteoblasts are protected from lead toxicity by transfection with DNA aptamers. The  
36 osteogenic development, which is decreased by lead exposure, is maintained by prior  
37 transfection of lead-binding DNA aptamers. Aptamers may be an effective strategy for  
38 the protection of human health in the face of increasing environmental toxicants.

39

40 **SYNOPSIS**

41 Lead remains a pervasive environmental contaminant with significant human health  
42 implications. This study investigates an entirely novel intervention for the problem of  
43 lead toxicity, using nucleic acid aptamers.

## 44 INTRODUCTION

45 Major water crises like the notorious case of Flint, MI<sup>1</sup>, and the ongoing problem  
46 of lead (Pb(II)) contamination in school water systems across the U.S.<sup>2</sup> make clear that  
47 lead exposure remains a pervasive public health problem. Lead causes  
48 neurodevelopmental anomalies in children<sup>3</sup> and increased risk of cardiovascular  
49 disease (CVD)<sup>4</sup>, renal damage, and neurological disease in adults<sup>5,6</sup>. Lead exposures  
50 are cumulative, and the neurologic damage caused is permanent. The molecular  
51 mechanism of lead toxicity is related to its ability to replace calcium in biological  
52 processes<sup>7</sup>. Lead enters cells through calcium channels and can interfere with calcium  
53 ion flow, which is a central mechanism of its neurotoxic effects<sup>8</sup>. Lead integrates into  
54 hydroxyapatite and can be stored for many years in bone<sup>9</sup>, leaching back into the body  
55 even after exposures are eliminated<sup>10,11</sup> and thus taking years or decades to be fully  
56 cleared from the body. Deposition of lead in the bone also interferes with bone cell  
57 signaling, maturation, and differentiation<sup>12-14</sup>, leading to impaired fracture healing<sup>15</sup> and  
58 increased risk of osteoporosis<sup>16,17</sup>.

59 Even very low levels of lead have been associated with health risks. Blood lead  
60 levels as low as 6.7 µg/dL in adults were associated with higher all-cause mortality, CVD  
61 mortality, and ischemic heart disease mortality<sup>18</sup>; even levels as low as 2 µg/dL  
62 represent a significant CVD risk<sup>19</sup>. Blood lead levels in children less than 5 µg/dL are  
63 associated with neurodevelopmental problems such as decreased academic  
64 achievement, decreased IQ, and increased incidence of attention-related and problem  
65 behaviors<sup>20</sup>. These findings suggest that the Centers for Disease Control and  
66 Prevention (CDC) guidelines for actionable blood lead levels, currently 3.5 µg/dL for  
67 children<sup>21</sup> and 5 µg/dL for adults<sup>22</sup>, are insufficient to protect against the negative health  
68 consequences of lead exposure. While intravenous EDTA chelation therapy is being  
69 explored to lower CVD risk in high-risk populations including diabetics<sup>23</sup>, there is not  
70 currently an approved, cost-effective, minimally invasive prophylactic or therapeutic  
71 intervention for chronic low-dose lead poisoning, which affects millions of people  
72 worldwide<sup>24</sup>.

73 Aptamers are short stretches of nucleic acids (<100 nucleotide single-stranded  
74 DNA or RNA molecules) that bind specifically to a target molecule or ion<sup>25</sup>. There are  
75 numerous aptamers currently in clinical trials for diseases ranging from various cancers  
76 to autoimmune conditions<sup>26</sup> and one aptamer drug (Macugen) is approved for the  
77 treatment of macular degeneration. Thus, as a therapeutic modality, aptamers have  
78 great promise<sup>27</sup>. Several studies have identified lead-binding aptamers with high  
79 sensitivity and specificity using Systematic Evolution of Ligands by Exponential  
80 Enrichment (SELEX)<sup>28</sup>. One such study identified an aptamer known as Pb7S with low  
81 micromolar affinity ( $1.60 \pm 0.16$  µM) for lead ions and reported minimal cross-reactivity  
82 to other ions<sup>29</sup>. Structural analyses suggest that lead may associate with nucleic acids  
83 through G-quadruplex (G4) structures<sup>30</sup>, though the mechanism of lead ion interaction  
84 for Pb7S has not been determined. Most lead-binding aptamers, including Pb7S, have

85 been developed for the purpose of lead detection in environmental and biological  
86 samples<sup>28</sup>. Whether lead-binding aptamers could be used clinically as specific lead ion  
87 chelators for the prophylactic or therapeutic treatment of lead poisoning has not yet  
88 been reported.

89 The nematode *Caenorhabditis elegans* is a ~1 mm transparent soil organism that  
90 has been used as a laboratory model organism for decades. The well-established  
91 genetic tools, facile imaging, rapid life cycle (~2 weeks), ease of maintenance, and  
92 complex-yet-mapped neural network<sup>31,32</sup> make *C. elegans* an ideal organism for a broad  
93 array of topics from aging<sup>33</sup> to neurodegeneration<sup>34</sup> to behavior<sup>35</sup>. These features have  
94 made *C. elegans* an ideal model organism for toxicology studies as well. Meta analyses  
95 have revealed that *C. elegans* toxicology studies have been just as predictive of  
96 adverse human outcomes and mechanisms of toxicity as rodent studies<sup>36</sup>, and yet can  
97 be performed at a fraction of the expense in time and resources.

98 Here we show, using a *C. elegans* model, that lead-chelating DNA and RNA  
99 aptamers applied in the presence of lead protect the animals from reproductive and  
100 behavioral toxicity. Both DNA and RNA versions of the aptamers are effective, and the  
101 protective effect is specific to lead and to the aptamer sequence. Further, using both  
102 HEK293 and primary murine osteoblast culture models, we show that aptamers protect  
103 cultured cells from lead toxicity, and protect osteoblastic function. The results suggest  
104 aptamer-based chelation could be further developed as a prophylactic or therapeutic  
105 strategy for human exposures to toxic metals.

106 **RESULTS**

107 *Lead Ions Interact Specifically with Lead-Binding ssDNA Aptamers*

108 The lead-binding single stranded (ss)DNA aptamer Pb7S (Table 1 and  
 109 Supplementary Table S1) has been described previously<sup>29</sup>. This aptamer was originally  
 110 selected for use in a fluorescence-based detection assay for lead (Supplementary Fig.  
 111 S1)<sup>29</sup>. The aptamers were 5' end labeled with a fluor (fluorescein amidite, FAM), and  
 112 annealed to a shorter antisense strand with a 3' quencher (dabcyl, DAB), which  
 113 quenched the fluorescent output. Upon aptamer binding to lead ions, the quench strand  
 114 was released, resulting in a fluorescent signal. To confirm lead binding to the Pb7S  
 115 aptamer, we reproduced the fluorescence-based lead binding assay, testing  
 116 combinations of two flours (FAM and Yakima Yellow) and three quenchers (DAB, Black  
 117 Hole Quencher 1 (BHQ1), and Iowa Black (IAB)) (Supplementary Fig. S2). Using the  
 118 Yakima Yellow fluor, we found a statistically significant difference in fluorescence from  
 119 the no lead control at 20  $\mu$ M lead, indicating an interaction of lead with the aptamer. The  
 120 fluorescence detection system was highly sensitive to pH, with lower (pH 5.5) and  
 121 higher (pH 8.4) values resulting in a loss of dynamic range (Supplementary Fig. S3),  
 122 which we suspected was a caveat of using fluorescent detection, rather than a pH-  
 123 dependent association of lead with the aptamer.

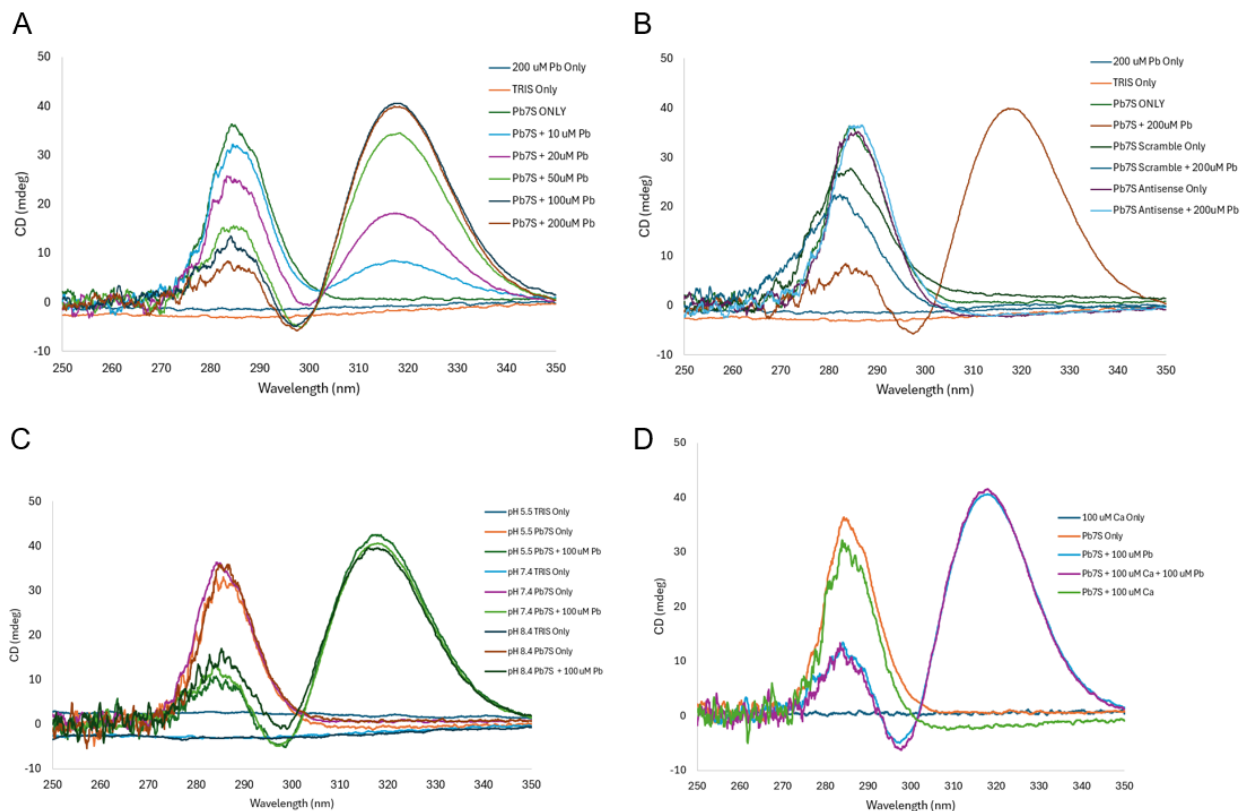
124 **Table 1: Sequences of Pb7 aptamers and controls.** Putative G-quadruplex residues shown in bold and underlined.

Aptamer	Length (nt)	Sequence
Pb7S	48	<u><b>GGG</b></u> <b>GACGAC</b> <u><b>GGC</b></u> <b>CAGGG</b> <u><b>GCT</b></u> <b>GTTCGTAC</b> <u><b>GG</b></u> <b>TTTTGTTCGAAGGTGTCGTCCCGA</b>
Pb7S antisense	48	TCGGGACGACACCTTCGACAAACCGTACGACAGCCCTGCCGTCTGTC
Pb7S scrambled	48	GCGGGCGATCTGCGGACGTTCTGAGCCTGACTGAGTGGGGACGCTGTA

125

126 Structural modeling predicts the formation of a G-quadruplex (G4) structure in the  
 127 Pb7S aptamer<sup>37</sup> (Table 1). Lead ions are known to assemble into G4s with high  
 128 affinity<sup>38</sup>, creating unique G4 signatures by circular dichroism (CD) spectroscopy<sup>39</sup>. To  
 129 confirm the specific interaction of the Pb7S aptamer with lead ions in a manner  
 130 independent from fluorescence detection, we applied CD to measure the lead-  
 131 dependent assembly of the G4 (Fig. 1). The unbound Pb7S aptamer, and antisense and  
 132 scrambled controls, displayed a strong CD maximum in a single peak at approximately  
 133 285 nm. The addition of lead ions to the Pb7S aptamer resulted in the concentration-  
 134 dependent appearance of a broad peak with a maximum at 317 nm (Fig. 1A).  
 135 Antisense aptamer and scrambled aptamer controls did not form the 317 nm peak in the  
 136 presence of lead (Fig. 1B). The formation of the peak at 317 nm was identical when the  
 137 pH of the solution used was 5.5 or 8.4, suggesting that the interaction is not particularly  
 138 sensitive to pH in this range (Fig. 1C). As lead mimics calcium within biological systems,  
 139 we investigated the binding of the Pb7S aptamer to calcium, and found no evidence of  
 140 binding of the Pb7S aptamer to calcium (Fig. 1D). Further, the presence of 100  $\mu$ M  
 141 calcium did not alter the formation of the 317 nm peak when lead was added

142 subsequently. From our CD experiments, we conclude that the Pb7S aptamer binds  
143 with high specificity to lead ions, not calcium.



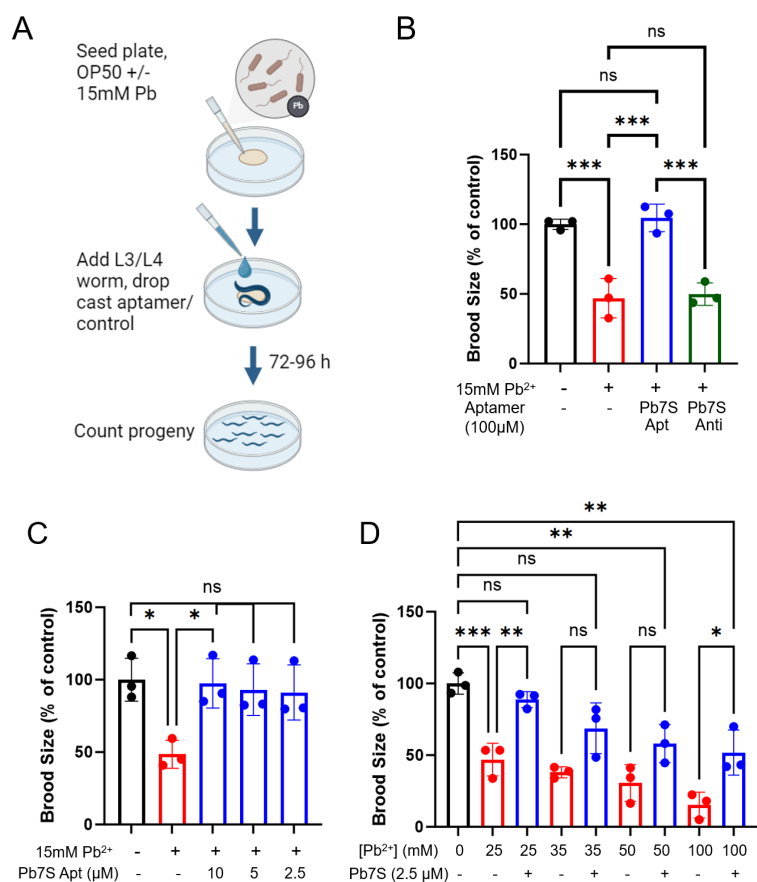
144  
145 **Figure 1. Pb7S binds specifically to lead ions.** A) Lead acetate (Pb) was added at indicated concentrations to 10  $\mu$ M samples of  
146 DNA aptamers (Pb7S) in 10 mM Tris pH 7.4. B) Pb7S antisense or scrambled aptamer controls (10  $\mu$ M) were mixed in 10 mM Tris  
147 pH 7.4 with or without 200  $\mu$ M Pb as indicated. The same graph of the Pb7S aptamer with 200  $\mu$ M Pb from panel A is overlaid in  
148 panel B for reference. C) 10  $\mu$ M samples of Pb7S aptamer, with or without Pb as indicated, were mixed in 10 mM Tris pH 5.5, 7.4, or  
149 8.4. D) 10  $\mu$ M samples of Pb7S aptamer, with or without 100  $\mu$ M Pb and/or 100  $\mu$ M calcium, as indicated, were mixed in 10 mM Tris  
150 pH 7.4. For all samples, CD measurement was performed on a Jasco J-1500, scanning at 100 nm/minute, 20  
151 accumulations/sample, from 250 nm – 350 nm in 0.1 nm intervals.

152

### 153 Reproductive Toxicity of Lead is Prevented by Pb-Binding ssDNA Aptamers

154 Lead has previously been shown to result in reproductive toxicity in *C. elegans*<sup>40–</sup>  
155 <sup>42</sup>, causing a dose-dependent decrease in brood size. These prior studies were  
156 conducted with animals exposed to metals by continuous growth in liquid cultures in  
157 multi-well plates. To better mimic dietary exposure to metals, we exposed our animals to  
158 metals by feeding. We first confirmed the dose-dependent decrease in brood size using  
159 our experimental feeding method. L3 stage animals were plated to NGM agar seeded  
160 with their food source OP50 *E. coli* mixed with lead acetate at concentrations from 0 –  
161 25 mM. We found by this method that 15 mM lead exposure mixed in the OP50 lawn  
162 was sufficient to reliably cause a minimum 50% decrease in brood size (Supplementary  
163 Fig. S4).

164 To determine whether chelation of lead ions with aptamers could reduce  
 165 reproductive toxicity, we employed three strategies to expose the animals to the  
 166 aptamer: feeding, soaking, and drop casting (Supplementary Fig. S5A, S6A, Fig. 2A).  
 167 The feeding strategy mixed the aptamers at the designated concentration into the  
 168 OP50, with or without lead, then animals were plated to this mixture and offspring were  
 169 counted (Supplementary Fig. S5A). The soaking strategy exposed animals to aptamers  
 170 in an aqueous solution for 2.5 hours, then the animals were moved to NGM plates  
 171 seeded with OP50 with or without lead (Supplementary Fig. S6A). For the drop casting  
 172 method, animals were plated to NGM plates containing OP50 with or without lead, then  
 173 10  $\mu$ L of aptamer at the indicated concentration was dropped onto the animal (Fig. 2A).  
 174 In all cases, the *C. elegans* cuticle is not permeable to the aptamer, and thus ingestion  
 175 of the aptamer is the predicted mechanism of exposure.



176

177

178 **Figure 2. Pb7S ssDNA aptamers protect *C. elegans* from reproductive toxicity caused by lead.** A) Schematic overview of the  
 179 drop casting experimental method. B) Brood size assay. L3/L4 animals were fed 15 mM lead acetate mixed with OP50. ssDNA  
 180 aptamers or water control were drop cast onto animals as indicated at 100  $\mu$ M. Brood size was assessed by counting total offspring  
 181 at 96 h. Apt, aptamer. Anti, antisense. One-way ANOVA  $P < 0.0001$ . C) Titration of the Pb7S aptamer. ssDNA aptamers were applied  
 182 using the drop cast method, and brood sizes determined at 96 h. One-way ANOVA  $P = 0.0149$ . D) Titration of lead concentration.  
 183 Lead acetate was mixed with OP50 at the indicated concentrations, then 2.5  $\mu$ M of Pb7S was drop cast onto animals. Brood sizes  
 184 were determined at 96 h. One-way ANOVA  $P < 0.0001$ . Data in all panels are presented as the mean of three experimental replicates  
 185 ( $n = 3$ ), wherein each overlaid point represents the experimental average of three technical replicates. Error bars are  $\pm$  S.E.M. \*\*\*  
 186  $P < 0.001$ , \*\*  $P < 0.005$ , \*  $P < 0.05$ , ns not significant, by one-way ANOVA with Tukey's post-hoc tests for multiple comparisons.

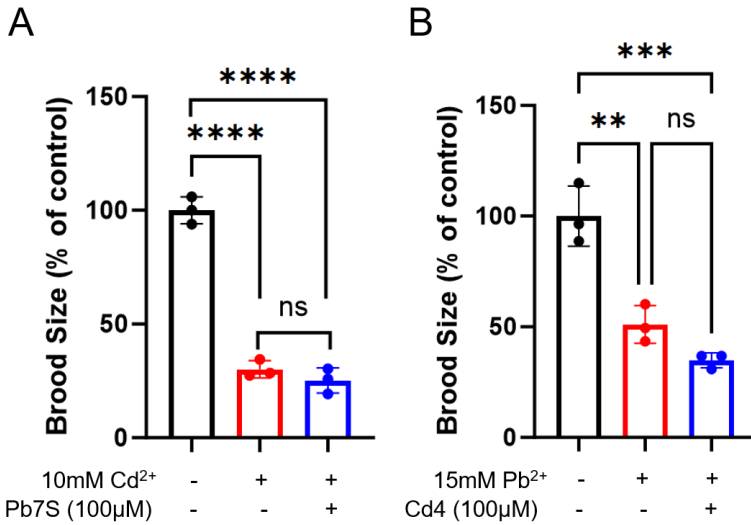
187



188 By all three exposure methods, we find exposure to the Pb7S aptamer, but not  
189 the antisense (reverse complement) aptamer or scrambled controls, results in a normal  
190 brood size (Supplementary Fig. S5, S6, Fig. 2B). To further confirm these results, we  
191 examined the original longer form of the Pb7S aptamer (known as Pb7) as well as the  
192 long and short forms of a second lead-binding aptamer identified by known as Pb14<sup>29</sup>,  
193 using the soaking method. Both the Pb7 and Pb14 aptamers, in their long and short  
194 forms, were effective in preventing the lead-associated decrease in brood size using the  
195 soaking method (Supplementary Fig. S6). In these soaking experiments, a modest but  
196 significant protective effect of the antisense strands was observed. We observed no  
197 effect of the Pb7, Pb7S, Pb14 or Pb14S aptamers, or their antisense sequences, on the  
198 reproductive toxicity of manganese<sup>41,42</sup> (Supplementary Fig. S6). The drop casing  
199 method proved to be more robust than feeding, and less toxic to the animals than  
200 soaking, so we continued with that method.

201 To thoroughly examine the protective effect of the Pb7S aptamer, we tested the  
202 aptamer at a range of both aptamer and lead concentrations using the drop casting  
203 method. The minimum effective concentration of aptamer required to achieve full  
204 protection from exposure at 15mM lead acetate was 2.5  $\mu$ M (Fig. 2C). At 2.5  $\mu$ M  
205 treatment, significant protection of animals was observed up to 100 mM lead acetate  
206 (Fig. 2D). Therefore, we have demonstrated the lead-specific, dose-dependent  
207 protection of animals from ingested lead toxicity by exposure to lead-binding ssDNA  
208 aptamers using multiple application methods.

209 Our feeding and soaking experiments determined there was no effect of the  
210 aptamers on manganese toxicity (Supplementary Fig. S5, S6). Manganese is a divalent  
211 cation and an essential trace element with well-established biological roles<sup>43</sup>; cadmium,  
212 like lead, is a divalent cation with no known biological role and has similarly been  
213 strongly correlated with cardiovascular disease risk<sup>44</sup>. To examine the specificity of the  
214 Pb7S aptamer in protecting *C. elegans* from reproductive lead toxicity, we determined  
215 that feeding of 10 mM cadmium caused an ~50% decrease in brood size  
216 (Supplementary Fig. S7), then tested the ability of the lead-binding Pb7S aptamer to  
217 rescue the cadmium-induced reproductive toxicity. The Pb7S aptamer had no effect on  
218 cadmium-induced reproductive toxicity (Fig. 3A). Several cadmium-binding aptamers  
219 have been described in the literature<sup>45,46</sup>, with nanomolar affinities to cadmium (34.5 nM  
220 for Cd-4<sup>46</sup>). When the Cd-4 (Fig. 3B) or Cd2-2 (Supplementary Fig. S8) aptamers were  
221 applied in our brood size assay, we found no effect on the reproductive toxicity caused  
222 by lead. We conclude that the lead-binding aptamers are specific for lead, as they had  
223 no effect on the reproductive toxicity of manganese or cadmium, in addition to published  
224 evidence that the aptamers are highly specific for their target ions<sup>29,45,46</sup>.



225

226

227

228

229

230

231

232

233

**Figure 3. Pb7S aptamer is specific for lead and does not protect against cadmium toxicity.** A) The Pb7S aptamer does not protect *C. elegans* from cadmium toxicity. 10mM cadmium chloride was mixed with OP50, and water or Pb7S aptamer was drop cast onto animals as indicated, then brood size assays were performed as described. One-way ANOVA  $P < 0.0001$ . B) The cadmium-binding Cd4 aptamer does not protect *C. elegans* from lead toxicity. 15 mM lead acetate was mixed with OP50, and the Cd4 aptamer or water control was drop cast onto animals as indicated, then brood size assays were performed as described. One-way ANOVA  $P = 0.0004$ . All data are presented as the mean of three experimental replicates ( $n = 3$ ), wherein each overlaid point represents the experimental average of three technical replicates. Error bars are  $\pm$  S.E.M. \*\*\*\*  $P < 0.0001$ , \*\*\*  $P < 0.001$ , \*\*  $P < 0.005$ , ns not significant, by one factor ANOVA with Tukey's post-hoc tests for multiple comparisons.

234

### 235 Behavioral Toxicity of Lead is Prevented by Pb-Binding ssDNA Aptamers

236

237

238

239

240

241

242

243

244

245

246

247

248

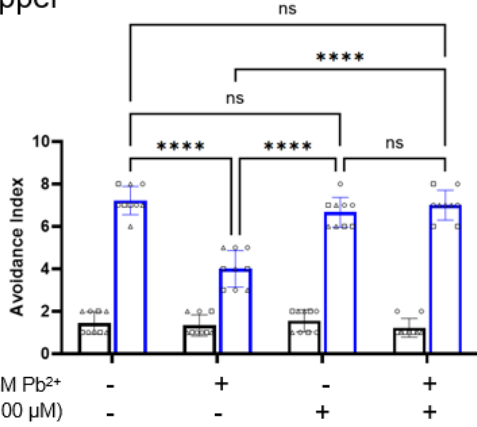
249

250

251

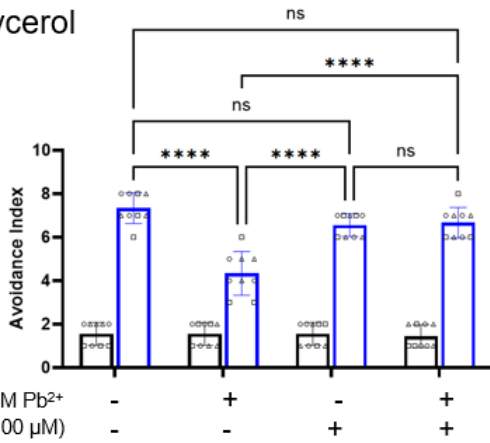
Early lead exposure in children is well established to result in developmental neurotoxicity<sup>3</sup>. We therefore sought to employ a model of developmental neurotoxicity in the form of a behavioral assay in our *C. elegans* model. *C. elegans* are known to move away from aversive cues, a pattern of behavior known as avoidance<sup>47</sup>. To determine whether lead exposure negatively impacted *C. elegans* avoidance behavior during larval development, we exposed L1 stage worms to 15 mM lead acetate and allowed them to develop to the L3/L4 stage in the presence of lead, then tested their avoidance of three known noxious cues, all of which are known to require the function of the ASH neurons<sup>48</sup>; copper, glycerol, and quinine. In all cases, lead exposure during larval development resulted in a dampened avoidance response to all noxious cues (Fig. 4A-C, blue bars). Exposure to the aptamer without lead did not affect the normal avoidance behavior. When the animals were exposed to the Pb7S aptamer in addition to the lead, we observed a restoration of the normal avoidance behavior. Animals in all experiments exposed to a solvent control were not responsive, as expected (Fig. 4A-C, black bars). These results suggest that the aptamer protects the animals from lead-induced behavioral toxicity during development.

A. copper



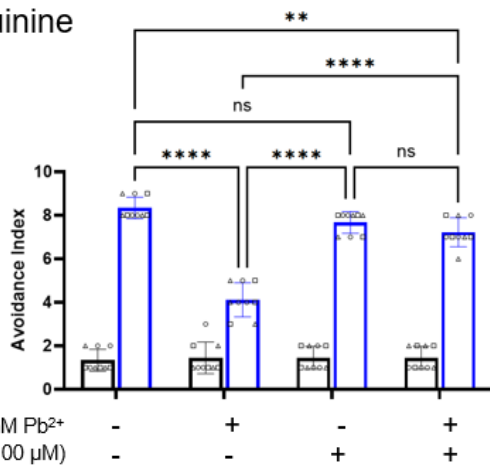
252

B. glycerol



253

C. quinine



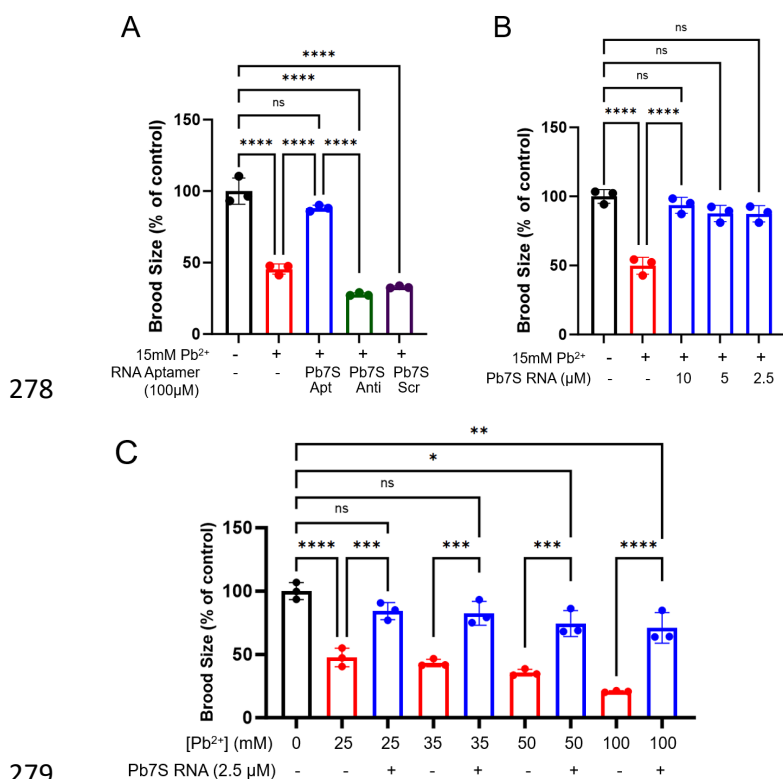
254

255

256 **Figure 4. The Pb7S DNA aptamer protects *C. elegans* from developmental lead neurotoxicity.** Animals were exposed to  
 257 noxious chemical cues copper chloride (A), glycerol (B) and quinine (C) (blue bars) or a water solvent control (black bars) and  
 258 observed for reversal of forward motion as described in Methods. For all panels,  $P < 0.0001$  by two-way ANOVA. Overlaid points  
 259 indicate 9 biological replicates, containing 10 animals tested per replicate, for a total of 90 animals tested. Replicates tested on the  
 260 same day are indicated with matching symbols.  $N = 9$ . Error bars are  $\pm$  S.E.M. \*\*\*\*  $P < 0.0001$ , \*\*  $P < 0.005$ , ns not significant, by two-  
 261 way ANOVA with Tukey's post-hoc tests for multiple comparisons.

262 Reproductive Toxicity of Lead is Prevented by Pb-Binding ssRNA Aptamers

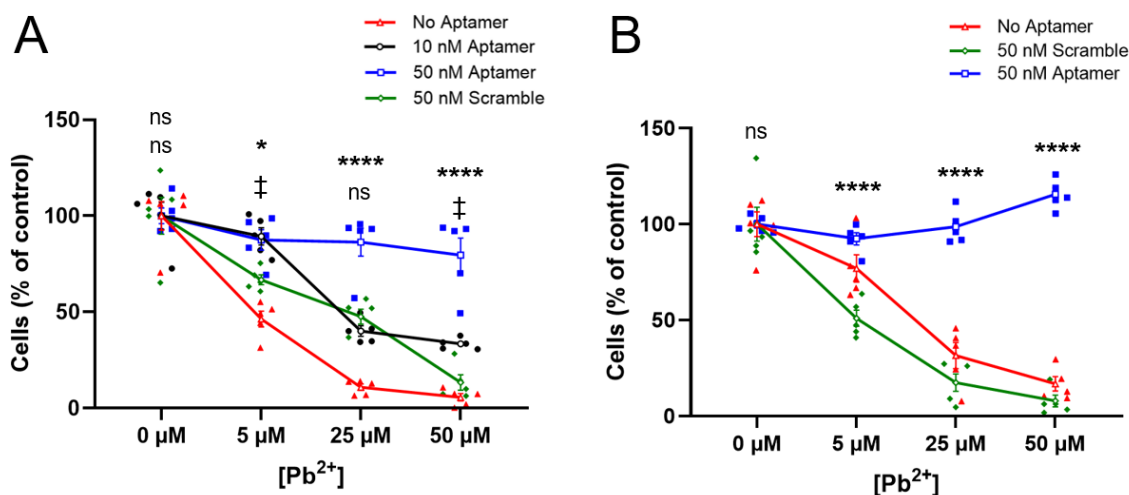
263 Modified RNAs (siRNAs and mRNAs) have been approved in the U.S. for  
 264 therapeutic and prophylactic uses<sup>49</sup> and are a promising treatment modality<sup>26,27</sup>. To  
 265 determine whether an RNA version of the Pb7S aptamer could also efficiently protect *C.*  
 266 *elegans* from reproductive toxicity, we repeated our brood size assays using RNA  
 267 versions of Pb7S and scrambled controls using the drop casting method. RNA aptamers  
 268 result in protection of animals from lead-induced reproductive toxicity, whereas  
 269 scrambled and antisense controls have no effect on brood size (Fig. 5A). To examine  
 270 the protective range of the RNA Pb7S aptamer, we tested the aptamer at a range of  
 271 both aptamer and lead concentrations. The minimum effective concentration of the RNA  
 272 aptamer required to achieve full protection from exposure at 15 mM lead acetate was  
 273 2.5  $\mu$ M (Fig. 5B). At 2.5  $\mu$ M treatment, significant protection of animals was observed up  
 274 to 100 mM lead acetate (Fig. 5C). These ranges were identical to those revealed in our  
 275 ssDNA Pb7S aptamer testing (Fig. 2C, 2D). We conclude that ssRNA Pb7S aptamers  
 276 are equally as effective as ssDNA aptamers in protecting *C. elegans* from reproductive  
 277 toxicity.



280 **Figure 5. Pb7S ssRNA aptamers protect *C. elegans* from reproductive toxicity.** A) Brood size assay. L3/L4 animals were fed  
 281 15mM lead acetate mixed with OP50. ssRNA aptamers or water control were drop cast onto animals as indicated at 100  $\mu$ M. Brood  
 282 size was assessed by counting total offspring at 96 h. Apt, aptamer. Anti, antisense. Scr, scrambled control. One-way ANOVA  
 283  $P < 0.0001$ . B) Titration of the Pb7S ssRNA aptamer. Aptamers were applied using the drop cast method, and brood sizes determined  
 284 at 96 h. One-way ANOVA  $P < 0.0001$ . C) Titration of lead concentration. Lead acetate was mixed with OP50 at the indicated  
 285 concentrations, then 2.5  $\mu$ M of Pb7S RNA was drop cast onto animals. Brood sizes were determined at 96 h. One-way ANOVA  
 286  $P < 0.0001$ . Data in all panels are presented as the mean of three experimental replicates ( $n=3$ ), wherein each overlaid point  
 287 represents the experimental average of three technical replicates. Error bars are  $\pm$  S.E.M. \*\*\*\*  $P < 0.0001$ , \*\*\*  $P < 0.001$ , \*\*  $P < 0.005$ ,  
 288 \*  $P < 0.05$ , ns not significant, by one-way ANOVA with Tukey's post-hoc tests for multiple comparisons.

289 Toxicity of Lead in Cultured Cells is Prevented by Pb-Binding ssDNA Aptamers

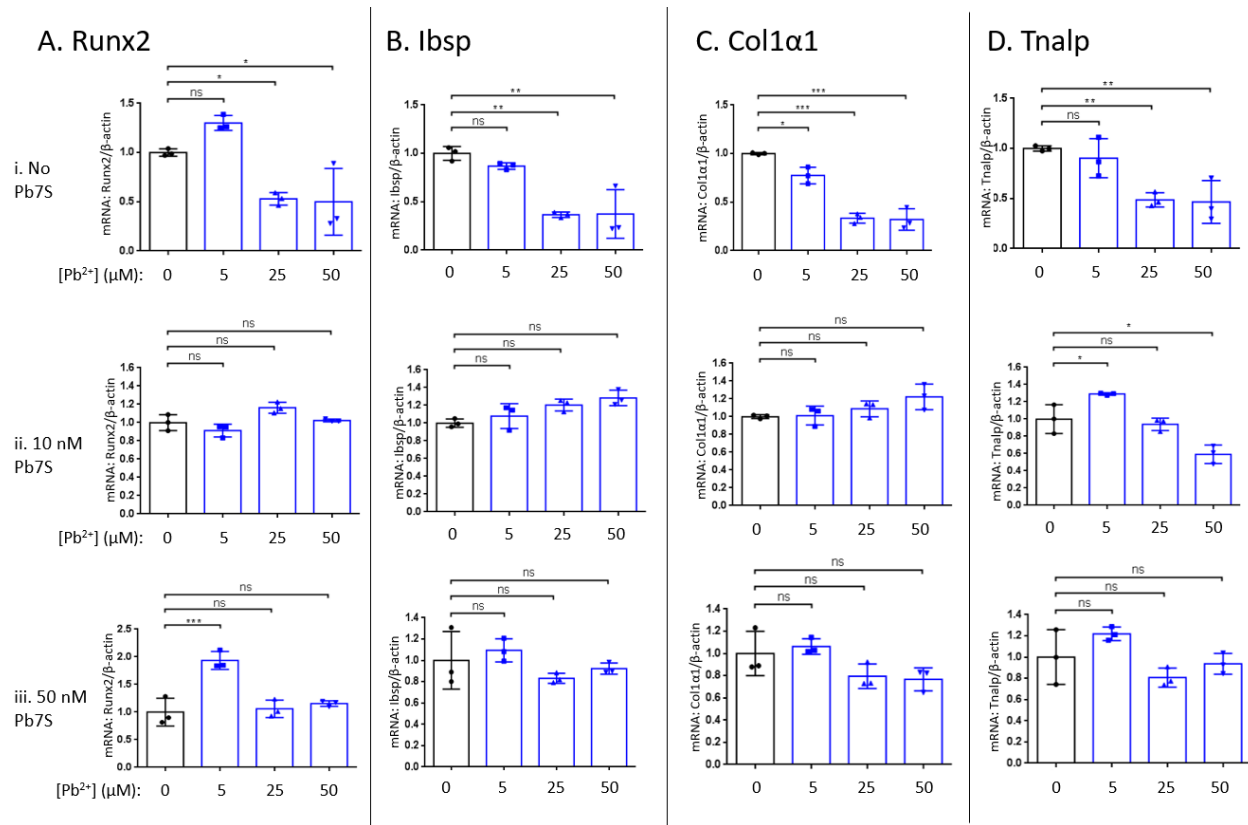
290 To determine whether ssDNA Pb7S aptamer could protect mammalian cells from  
 291 lead toxicity, we used cell proliferation assays to measure the effect of lead on cultured  
 292 cell growth. We investigated the effects of lead exposure on cell proliferation in HEK293  
 293 cells and primary murine calvarial osteoblasts over a concentration range from 0 to 50  
 294  $\mu\text{M}$ , and assessed the ability of aptamers to mitigate lead toxicity. Calvarial osteoblasts  
 295 were isolated from calvaria of wildtype neonates at postnatal day 5. We observed a  
 296 substantial and dose-dependent reduction in cell proliferation at 48 h of lead exposure  
 297 in both cell types (Fig. 6A, 6B). Transfection of the Pb7S aptamer at concentrations of  
 298 10 nM or 50 nM partially or completely, respectively, protected the cells from cytotoxicity  
 299 and preserved proliferation, relative to transfection of the scrambled control.



300  
 301 **Figure 6. ssDNA Pb7S aptamers protect cultured HEK293T and primary calvarial osteoblasts from lead toxicity.** HEK293 (A)  
 302 or primary calvarial osteoblasts (B) were transfected with 10 nM (black line and symbols) or 50 nM (blue line and symbols) Pb7S  
 303 aptamer, or 50 nM scrambled control (green line and symbols), or mock transfected (no aptamer, red line and symbols), then  
 304 exposed to lead concentrations as indicated.  $P < 0.0001$  by two-way ANOVA for each panel. Data in both panels are presented as the  
 305 mean of five experimental replicates ( $n=5$ ), wherein each overlaid point represents the experimental average of 3-4 technical  
 306 replicates. Bars are  $\pm$  S.E.M. \*\*\*\*  $P < 0.0001$ , \*  $P < 0.05$ , for comparison between 50 nM Pb7S aptamer and 50 nM scramble  
 307 conditions; ‡  $P < 0.05$ , for comparison between 10 nM Pb7S aptamer and 50 nM scramble control; ns not significant, by two-way  
 308 ANOVA with Tukey's post-hoc tests for multiple comparisons.

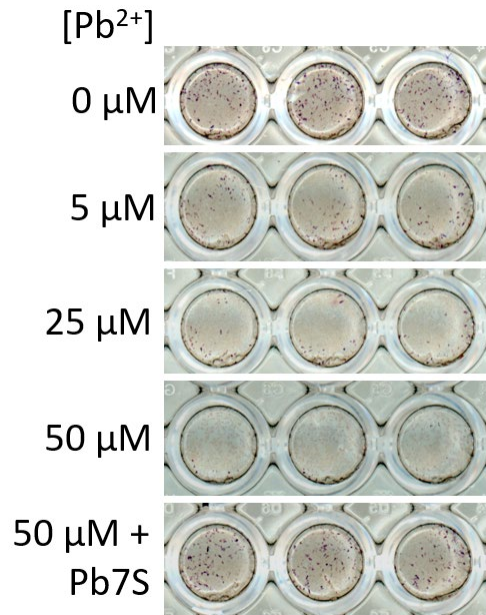
309 To establish the functional toxicity of lead in osteogenic differentiation of cultured  
 310 primary calvarial osteoblasts, the expression of osteogenic marker genes, such as  
 311 Runx2 (Fig. 7A), bone sialoprotein (Ibsp, Fig. 7B), type I collagen  $\alpha$  1 (Col1 $\alpha$ 1, Fig. 7C),  
 312 and tissue-nonspecific alkaline phosphatase (Tnlp, Fig. 7D) were examined<sup>50,51</sup>. Cells  
 313 were treated with different concentrations of lead over a 6-day period, with or without  
 314 the transfection of the Pb7S aptamer, prior to RNA extraction and analysis by qPCR.  
 315 We observed a significant inhibition of expression of these osteogenic genes (Fig. 7Ai –  
 316 Di) in response to lead exposure. Notably, when cells were first transfected with 10 nM  
 317 Pb7S aptamer (Fig. 7Aii-Dii), gene expression was not affected by the exposure to lead,  
 318 effectively rescuing the expression of these genes from the inhibitory effects of lead.

319 This protective effect was consistently replicated, and in the case of Runx2, enhanced,  
 320 when cells were transfected with a higher aptamer concentration of 50 nM (Fig. 7Aiii-  
 321 Diii). These findings highlight the aptamer's capacity to prevent the suppression of  
 322 osteogenic gene expression caused by lead, and to counteract the negative impact of  
 323 lead on these critical factors in osteoblast development and differentiation.



324  
 325 **Figure 7. Changes in osteogenic gene expression caused by lead are prevented by the Pb7S aptamer.** Primary calvarial  
 326 osteoblasts were mock transfected (i) or transfected with the Pb7S DNA aptamer at 10 nM (ii) or 50 nM (iii), and treated with lead  
 327 concentrations as indicated, then RNA was extracted and analyzed by qRT-PCR for osteogenic gene markers Runx2 (A), Ibsp (B),  
 328 Col1a1 (C) or Tnalp (D). N=3. Error bars are  $\pm$  S.E.M. \*\*\* P<0.001, \*\* P<0.005, \* P<0.05, ns not significant, by student's t test  
 329 versus 0  $\mu$ M lead controls.

330  
 331 We next examined alkaline phosphatase (ALP) activity in primary calvarial osteoblasts,  
 332 which is a hallmark of differentiated, active osteoblasts<sup>52</sup>. In alignment with the gene  
 333 expression results, increasing lead exposure resulted in decreased ALP activity (Fig. 8),  
 334 suggesting that lead exposure negatively impacts osteogenic differentiation. However,  
 335 transfection of the ssDNA Pb7S aptamer effectively preserved ALP function and  
 336 increased ALP staining. The results suggest that both osteoblast survival and function are  
 337 protected from the toxic effects of lead by the presence of the aptamer.



338

339 **Figure 8. Lead induced decrease in osteogenic differentiation is prevented by exposure to the ssDNA Pb7S aptamer.**  
 340 Primary murine calvarial osteoblasts were transfected with Pb7S DNA aptamer as described, or a mock transfection control, then  
 341 exposed to lead acetate concentrations as indicated. ALP activity was assessed by Fast Blue staining. Wells shown are technical  
 342 replicates.

343

344

345 **DISCUSSION**

346 The current standard of treatment for lead toxicity is chelation therapy with oral  
 347 medication, or EDTA chelation by intravenous administration<sup>53</sup>. However, these  
 348 therapies are typically only offered in the case of extremely high lead levels (blood lead  
 349 levels above 45  $\mu\text{g}/\text{dL}$  for children and 70  $\mu\text{g}/\text{dL}$  for adults<sup>53</sup>), despite the fact that much  
 350 lower levels are associated with negative health consequences, as discussed  
 351 above<sup>18,19</sup>. The recommended course of action for lower blood lead levels (3.5 – 45  
 352  $\mu\text{g}/\text{dL}$ ) is to continue to monitor the lead levels of the patient and attempt to identify and  
 353 eliminate the source of contamination<sup>53</sup>. Again, this course of action cannot reverse  
 354 permanent neurologic damage, nor can it prevent the accumulation of lead in bones.  
 355 Many lead exposures are via ingestion from environmental sources: water, food, or  
 356 incidental ingestion of contaminated dust or paint chips<sup>53</sup>. When the water or working  
 357 conditions are to blame, it may be difficult or impossible to eliminate lead from the  
 358 environment completely. This is particularly true for low-income families. Analysis of the  
 359 NHANES data from 2015-2018 revealed that Hispanic, Black, and low-income children  
 360 of all races (ages 1-5) were significantly more likely to have elevated blood lead levels  
 361 as compared to the national average of all races/incomes<sup>20</sup>. The neurotoxic effects of  
 362 lead are permanent, leading to life-long cognitive deficits in these children and creating  
 363 a disease burden that is borne disproportionately by racially diverse and low-income

364 communities<sup>54</sup>. Therefore, there is not only an urgent need but an environmental justice  
365 obligation to develop accessible and cost-effective methods to protect people from lead.

366 In this work, we demonstrate that the Pb7S aptamer binds with sensitivity and  
367 specificity to lead ions, and can efficiently chelate these ions to inhibit their toxicity.  
368 ssDNA aptamers applied to *C. elegans* protected animals from reproductive toxicity and  
369 behavioral toxicity caused by lead ingestion. The aptamers are specific to lead, and do  
370 not affect cadmium toxicity or manganese toxicity. The protective effect of Pb7S was  
371 observed with three different methods of aptamer delivery: feeding, soaking, and drop  
372 casting. Our CD spectroscopy experiments, in alignment with the literature<sup>30,38</sup>, suggest  
373 that Pb7S forms a stable complex with lead ions, and that there is no discernible  
374 interference of the interaction by calcium. The dramatic shift in the CD spectra of lead in  
375 complex with Pb7S supports the possibility that the aptamer chelates lead in a stable  
376 G4 structure, though additional investigation will be needed to determine the specific  
377 structure and binding kinetics of the complex. Finally, exposure of *C. elegans* to the  
378 Pb7S aptamer is protective against lead toxicity. However, future studies are needed to  
379 examine the protection mechanism, including ascertaining intracellular lead levels and  
380 translation of the effects to whole vertebrate animals.

381 Our studies revealed that RNA versions of the Pb7S aptamer were equally as  
382 effective as DNA aptamers in providing a protective effect in our reproductive toxicity  
383 assays. This raises the possibility that RNA-based aptamers could be developed for  
384 clinical use as an alternative to intravenous sodium edetate (EDTA) therapy for lead  
385 poisoning. These aptamer-based chelation over chemical chelators like EDTA could  
386 improve specificity for lead ions leading to decreased calcium excretion<sup>55</sup>, as well as  
387 administration (a subcutaneous injection<sup>56,57</sup> at home versus intravenous therapy in a  
388 clinic). Modified RNAs are increasingly being used as prophylactics and therapeutics in  
389 the form of mRNA vaccines, antisense oligonucleotides (ASOs), and small interfering  
390 (si)RNAs, and their impact is expected to increase rapidly and significantly<sup>49</sup>. Aptamers  
391 are known from human studies to be generally safe and efficiently excreted by the  
392 kidneys<sup>58</sup>, which is a drawback for ASOs or siRNAs used therapeutically but in the  
393 context of eliminating lead ions or other toxins may be an asset.

394 In human HEK293 cells and murine calvarial osteoblasts, we demonstrated the  
395 protective effects of the Pb7S aptamer on cell proliferation, osteogenic gene expression,  
396 and osteogenic differentiation. In a rat model of developmental lead exposure,  
397 dimercaptosuccinic acid (DMSA) chelation partially reversed negative changes in bone  
398 microarchitecture and osteogenic markers associated with lead exposures<sup>59</sup>, which  
399 suggests that the decreased osteogenic potential associated with lead toxicity may be  
400 reversible with chelation. Our results suggest therapeutic potential of aptamers to  
401 protect cells and organ systems from lead toxicity. Whether aptamers could be used to  
402 reverse some of its toxic effects is unknown, but is an important future avenue of  
403 investigation.



404 A 10-year, large scale clinical trial (the Trial to Assess Chelation Therapy, TACT)  
405 studied the use of intravenous chelation therapy with EDTA to reduce the incidence of  
406 repeat adverse events and death in patients that had already suffered one heart  
407 myocardial infarction (MI)<sup>60</sup>. The study found that heavy metal chelation resulted in an  
408 18% decrease in repeat adverse CVD events. In diabetic patients, EDTA chelation  
409 reduced repeat CVD events by 41%<sup>61</sup>. Importantly, the study participants were not  
410 selected based on blood lead levels; they were patients who had MI previously. The  
411 implication is that our standard lifetime exposures to metals, lead and cadmium in  
412 particular<sup>4</sup>, are increasing our risk of heart disease, and that decreasing these metals in  
413 our system results in a decreased risk of CVD and death. Aptamer-based chelation  
414 strategies will require further research before they are ready for the clinic. However,  
415 given that over 14% of the U.S. population is estimated to be diabetic<sup>62</sup> and that CVD is  
416 the number one leading cause of death in the U.S.<sup>63</sup>, the potential impact of decreasing  
417 toxic heavy metal absorption, at least in part by employing aptamers, cannot be  
418 overstated.

419

## 420 **MATERIALS AND METHODS**

### 421 **Reagents, cell lines, and materials**

422 Aptamer sequences are listed in Supplementary Table S1. All aptamers were  
423 synthesized as standard desalted single-stranded DNA or RNA oligonucleotides by IDT-  
424 DNA (Coralville, IA, and Research Triangle Park, NC, USA). Wildtype N2 *C. elegans*  
425 were obtained from the Caenorhabditis Genetics Center (University of Minnesota, MN),  
426 and were used for all experiments. N2 animals were maintained on nematode growth  
427 media (NGM) plates and fed with OP50 *E. coli*. HEK293 cells were obtained from the  
428 American Type Culture Collection in Rockville, Maryland. These cells were cultured in  
429 Dulbecco's Modified Eagle Medium (DMEM) from Corning, with the addition of 10%  
430 Fetal Bovine Serum (FBS), 2 mM L-glutamine, 1% penicillin/streptomycin, and 1%  
431 nonessential amino acids, all of which were also provided by Corning. The cells were  
432 maintained at 37°C in a humidified environment with 5% CO<sub>2</sub>.

### 433 **Primary murine calvarial osteoblast cell culture**

434 Primary calvarial osteoblasts were isolated from calvaria of 5-day-old neonates using  
435 collagenase type II (50 mg/ml, Worthington, LS004176)/dispase II (100 mg/ml,  
436 Roche, 10165859001). Osteoblasts were maintained in alpha-minimal essential medium  
437 (aMEM) (Gibco) containing 10% FBS (Gibco), 2mM L-glutamine (Corning), 1%  
438 penicillin/streptomycin (Corning), and 1% nonessential amino acids (Corning) and  
439 differentiated with ascorbic acid (200 uM, Sigma, A8960). and β-glycerophosphate  
440 (10 mM, Sigma, G9422). To induce osteogenic differentiation, the growth media was  
441 supplemented with ascorbic acid (200 mM, Sigma, A8960) and beta-glycerophosphate  
442 (10 mM, Sigma, G9422).

### 443 **Osteoblast differentiation analysis**

444 To assess osteoblast differentiation, alkaline phosphatase (ALP) activity was  
445 determined as described previously<sup>52</sup>. In brief, differentiated osteoblasts were washed  
446 with phosphate-buffered saline (PBS) and incubated with a solution containing 6.5 mM  
447 Na<sub>2</sub>CO<sub>3</sub>, 18.5 mM NaHCO<sub>3</sub>, 2 mM MgCl<sub>2</sub>, and a phosphatase substrate (Sigma,  
448 S0942). ALP activity was measured using a spectrophotometer. ALP staining was  
449 performed using Fast Blue (Sigma, FBS25) and Naphthol AS-MX (Sigma, 855) after  
450 fixation in 10% neutral formalin buffer.<sup>63</sup>

### 451 **Lead treatment and aptamer transfection**

452 Aptamer transfections were conducted using Lipofectamine RNAi MAX reagent in Opti-  
453 MEM®I Reduced Serum Medium (from Invitrogen, Carlsbad, CA, USA) following the  
454 manufacturer's protocol. Calvarial osteoblasts were plated at a density of 5x10<sup>4</sup> cells  
455 per well in a 12-well plate. One day later, the cells were exposed to either lead acetate  
456 alone at indicated concentrations, or a combination of lead and aptamers (10nM, 25nM  
457 and 50nM) in Opti-MEM (reduced serum medium) using Lipofectamine RNAi MAX  
458 reagent from Invitrogen for 6 hours. After 6 hours, the culture medium was changed to a

459 differentiation medium for a period of 6 days. The differentiation medium was changed  
460 every 2 days. Cells were harvested for RNA isolation after 6 days of differentiation.

#### 461 **Cell proliferation assays**

462 The Alamar Blue assay was performed in 96-well plates to assess cell proliferation  
463 according to the manufacturer's instructions. Each well was initially seeded with a cell  
464 density ranging from 5,000 to 10,000 cells. After a 24-hour incubation, the cells were  
465 exposed to various concentrations of Pb (0, 0.25 $\mu$ M, 0.5 $\mu$ M, 1 $\mu$ M, 5 $\mu$ M, 10 $\mu$ M, 25 $\mu$ M  
466 and 50 $\mu$ M). Concurrently, the cells were transfected with three different concentrations  
467 of Aptamers (Apt) at 10nM, 25nM and 50nM. These treatments were applied for both 24  
468 and 48 hours. The culture medium was aspirated, and the cells were rinsed with  
469 phosphate-buffered saline (PBS). Then, cells were incubated with 100 $\mu$ l of tenfold  
470 diluted Alamar Blue solution (Invitrogen, DAL1100). After a 3-hour incubation period, the  
471 fluorescence of the Alamar Blue was measured at excitation and emission wavelengths  
472 of 575 and 595 nm using a Tecan Genios microplate reader. Measurements of cell  
473 viability using the Alamar Blue assay were taken 24 hours after the initial setup.

#### 474 **Quantitative RT-PCR analysis**

475 Total RNA was isolated from cells using QIAzol (QIAGEN) and cDNA was synthesized  
476 with 1 $\mu$ g of RNA using the High-Capacity cDNA Reverse Transcription Kit (Applied  
477 Biosystems). SYBR green chemistry was used for quantitative determination of the  
478 various mRNAs for Runx-2, Ibsp, Col1 $\alpha$ 1, Tnalp, and a housekeeping gene  $\beta$ -actin.  
479 Quantitative RT-PCR was performed using SYBR<sup>®</sup> Green PCR Master Mix (Bio-Rad)  
480 with CFX connect RT-PCR detection system (Bio-Rad).

#### 481 **Brood Size Assays**

482 NGM plates were seeded with 75  $\mu$ L of *E. coli* OP50, mixed with or without lead acetate  
483 concentrations as indicated (and/or ssDNA aptamers as indicated for the feeding  
484 method). One L3-L4 N2 wildtype aged-synchronized worm was plated onto each  
485 seeded plate. For the drop casting method, 10  $\mu$ L of aptamer solution (ssDNA or RNA)  
486 at the indicated concentration was applied to the animal by pipetting after plating. The  
487 brood size was determined at 72 or 96 hours as indicated.

#### 488 **Avoidance Assay**

489 Assays were performed as described previously<sup>48,64</sup>. Briefly, developmental plates  
490 containing 20 L1 N2 aged-synchronized worms were plated to NGM plates with or  
491 without 15 mM lead acetate, and with or without drop casting of 100  $\mu$ M Pb7S ssDNA  
492 aptamer, and incubated at 20°C for 72 hours where they developed to the L3/L4 stage.  
493 *C. elegans* from the developmental plate were transferred to an acclimation plate in the  
494 testing room and allowed to acclimate to the new plate for 30 minutes. A drop of either  
495 water (solvent control) or stimulus (1 M glycerol, 10 mM Copper (II) chloride dihydrate, 1  
496 mM quinine) was placed on the tail of forward moving animals, and their response was  
497 scored as either an avoidance response (two body bends of reverse motion), or no

498 response. The total number of avoidances was divided by the total number of drops to  
499 generate an avoidance index for that plate. This was repeated for at least 3 plates of 10  
500 animals each, over at least three different days.

501

## 502 **STATISTICAL ANALYSIS**

503 Statistical analyses were performed with GraphPad Prism software. All *C. elegans* and  
504 cell culture data were first analyzed by one-way or two-way ANOVA, as appropriate,  
505 followed by post-hoc testing as indicated in the figure legend. qRT-PCR results were  
506 analyzed by student's t tests.

507

## 508 **SUPPLEMENTARY INFORMATION**

509 Supplementary Figures 1 – 8, and Supplementary Table 1, are associated with this  
510 manuscript.

511

## 512 **DATA AVAILABILITY**

513 The data that support the findings of this study are available from the corresponding  
514 author upon reasonable request.

515

## 516 **ACKNOWLEDGEMENTS**

517 This work was supported in part by the generous philanthropy of Mr. Robert Ferrari of  
518 Northeast Water Solutions Inc. and Ferrari Engineering Inc. A.A. and S. Ramis de  
519 Ayreflor Reyes were supported in part by the Robert F. Ferrari '74 Graduate Research  
520 Fund. N.G.F is supported in part by seed grant funding and new faculty start-up funds  
521 from WPI. We thank Caroline Muirhead and Elizabeth DiLoreto for technical assistance  
522 and advice. J.H.S. is supported by NIH/NIAMS (R01AR068983, R21AR073331), the  
523 International FOP Association, AAVAA Therapeutics, and Dong-A ST.

524

## 525 **AUTHOR CONTRIBUTIONS**

526 A.A. and S. Ramis de Ayreflor Reyes performed all experiments with the following  
527 exceptions: A.A.J. performed HEK293 and murine osteoblast experiments; A.M.O.  
528 performed the cadmium toxicity curve; S. Reis performed behavioral toxicity on L3/L4 *C.*  
529 *elegans*; E.B. and N.G.F. performed CD spectroscopy experiments. Mentoring and  
530 supervision: J.H.S., A.A.S., J.S., N.G.F. Financial support: J.S. and N.G.F. Writing,  
531 original draft: N.G.F., A.A. and A.A.J. All authors contributed to editing and revision and  
532 have reviewed and approved the final manuscript.

533 **COMPETING INTERESTS**

534 N.G.F., A.A., and S. Ramis de Ayreflor Reyes have filed a patent application for the  
535 technology described herein. J.H.S. is a scientific co-founder of AAVAA Therapeutics  
536 and holds equity in this company. All other authors declare no competing interests.

537

538 **MATERIALS & CORRESPONDENCE**

539 Correspondence and material requests should be addressed to N.G.F, [nfarny@wpi.edu](mailto:nfarny@wpi.edu)

540

541

542

543

544 **REFERENCES**

545 1. Santucci, R. J. & Scully, J. R. The pervasive threat of lead (Pb) in drinking water:  
546 Unmasking and pursuing scientific factors that govern lead release. *Proceedings of the*  
547 *National Academy of Sciences* **117**, 23211–23218 (2020).

548 2. Rumpler, J. & Casale, M. *Get the Lead Out: Grading the States on Protecting Kids’*  
549 *Drinking Water at School*. [https://publicinterestnetwork.org/wp-](https://publicinterestnetwork.org/wp-content/uploads/2023/02/AME-GTLO-Report-Feb23-1.2.pdf)  
550 [content/uploads/2023/02/AME-GTLO-Report-Feb23-1.2.pdf](https://publicinterestnetwork.org/wp-content/uploads/2023/02/AME-GTLO-Report-Feb23-1.2.pdf) (2023).

551 3. Santa Maria, M. P., Hill, B. D. & Kline, J. Lead (Pb) neurotoxicology and cognition. *Appl*  
552 *Neuropsychol Child* **8**, 272–293 (2019).

553 4. Lamas, G. A. *et al.* Contaminant Metals as Cardiovascular Risk Factors: A Scientific  
554 Statement From the American Heart Association. *J Am Heart Assoc* e029852 (2023).

555 5. Ramírez Ortega, D. *et al.* Cognitive Impairment Induced by Lead Exposure during  
556 Lifespan: Mechanisms of Lead Neurotoxicity. *Toxics* **9**, 23 (2021).

557 6. Centers for Disease Control and Prevention. *Elevated Blood Lead Levels Among*  
558 *Employed Adults — United States, 1994–2012*. (2015).

559 7. Simons, T. J. Lead-calcium interactions in cellular lead toxicity. *Neurotoxicology* **14**, 77–  
560 85 (1993).

561 8. Rocha, A. & Trujillo, K. A. Neurotoxicity of low-level lead exposure: History, mechanisms  
562 of action, and behavioral effects in humans and preclinical models. *Neurotoxicology* **73**,  
563 58–80 (2019).

564 9. Pemmer, B. *et al.* Spatial distribution of the trace elements zinc, strontium and lead in  
565 human bone tissue. *Bone* **57**, 184–193 (2013).

- 566 10. Sánchez-Fructuoso, A. I. *et al.* Lead mobilization during calcium disodium  
567 ethylenediaminetetraacetate chelation therapy in treatment of chronic lead poisoning.  
568 *American journal of kidney diseases* **40**, 51–58 (2002).
- 569 11. Gulson, B. L., Mizon, K. J., Korsch, M. J., Palmer, J. M. & Donnelly, J. B. Mobilization of  
570 lead from human bone tissue during pregnancy and lactation—a summary of long-term  
571 research. *Science of the Total Environment* **303**, 79–104 (2003).
- 572 12. Sun, K. *et al.* Lead exposure inhibits osteoblastic differentiation and inactivates the  
573 canonical Wnt signal and recovery by icaritin in MC3T3-E1 subclone 14 cells. *Chem Biol*  
574 *Interact* **303**, 7–13 (2019).
- 575 13. Beier, E. E. *et al.* Heavy metal ion regulation of gene expression: mechanisms by which  
576 lead inhibits osteoblastic bone-forming activity through modulation of the Wnt/ $\beta$ -catenin  
577 signaling pathway. *Journal of Biological Chemistry* **290**, 18216–18226 (2015).
- 578 14. Al-Ghafari, A., Elmorsy, E., Fikry, E., Alrowaili, M. & Carter, W. G. The heavy metals lead  
579 and cadmium are cytotoxic to human bone osteoblasts via induction of redox stress.  
580 *PLoS One* **14**, e0225341- (2019).
- 581 15. Beier, E. E. *et al.* Inhibition of beta-catenin signaling by Pb leads to incomplete fracture  
582 healing. *Journal of Orthopaedic Research* **32**, 1397–1405 (2014).
- 583 16. Puzas, J. E. & Boyce, B. F. Chapter 22 - Metal ion toxicity in the skeleton: lead and  
584 aluminum. in *Principles of Bone Biology (Fourth Edition)* (eds. Bilezikian, J. P., Martin, T.  
585 J., Clemens, T. L. & Rosen, C. J.) 527–537 (Academic Press, 2020).  
586 doi:<https://doi.org/10.1016/B978-0-12-814841-9.00022-1>.
- 587 17. Lee, C. M. *et al.* Chronic lead poisoning magnifies bone detrimental effects in an  
588 ovariectomized rat model of postmenopausal osteoporosis. *Experimental and Toxicologic*  
589 *Pathology* **68**, 47–53 (2016).
- 590 18. Lanphear, B. P., Rauch, S., Auinger, P., Allen, R. W. & Hornung, R. W. Low-level lead  
591 exposure and mortality in US adults: a population-based cohort study. *Lancet Public*  
592 *Health* **3**, e177–e184 (2018).
- 593 19. Nawrot, T. S. & Staessen, J. A. Low-level environmental exposure to lead unmasked as  
594 silent killer. *Circulation* vol. 114 1347–1349 Preprint at (2006).
- 595 20. National Toxicology Program. *NTP MONOGRAPH ON HEALTH EFFECTS OF LOW-*  
596 *LEVEL LEAD*. (2012).
- 597 21. Ruckart, P. Z. *et al.* Update of the blood lead reference value—United States, 2021.  
598 *Morbidity and Mortality Weekly Report* **70**, 1509 (2021).
- 599 22. Centers for Disease Control and Prevention. *National Notifiable Diseases Surveillance*  
600 *System (NNDSS), Lead, Elevated Blood Lead Level*. (2016).
- 601 23. Lamas, G. A., Navas-Acien, A., Mark, D. B. & Lee, K. L. Heavy metals, cardiovascular  
602 disease, and the unexpected benefits of chelation therapy. *J Am Coll Cardiol* **67**, 2411–  
603 2418 (2016).

- 604 24. Larsen, B. & Sánchez-Triana, E. Global health burden and cost of lead exposure in  
605 children and adults: a health impact and economic modelling analysis. *Lancet Planet*  
606 *Health* **7**, e831–e840 (2023).
- 607 25. Ellington, A. D. & Szostak, J. W. Selection in vitro of single-stranded DNA molecules that  
608 fold into specific ligand-binding structures. *Nature* **355**, 850–852 (1992).
- 609 26. Nimjee, S. M. & Sullenger, B. A. Therapeutic aptamers: evolving to find their clinical  
610 niche. *Curr Med Chem* **27**, 4181–4193 (2020).
- 611 27. Di Ruscio, A. & de Franciscis, V. Minding the gap: Unlocking the therapeutic potential of  
612 aptamers and making up for lost time. *Mol Ther Nucleic Acids* **29**, 384–386 (2022).
- 613 28. Yang, D. *et al.* Aptamer-based biosensors for detection of lead(ii) ion: a review. *Analytical*  
614 *Methods* **9**, 1976–1990 (2017).
- 615 29. Chen, Y. *et al.* Selection of DNA aptamers for the development of light-up biosensor to  
616 detect Pb(II). *Sens Actuators B Chem* **254**, 214–221 (2018).
- 617 30. Kotch, F. W., Fettinger, J. C. & Davis, J. T. A Lead-Filled G-Quadruplex: Insight into the  
618 G-Quartet's Selectivity for Pb<sup>2+</sup> over K<sup>+</sup>. *Org Lett* **2**, 3277–3280 (2000).
- 619 31. White, J. G., Southgate, E., Thomson, J. N. & Brenner, S. The structure of the nervous  
620 system of the nematode *Caenorhabditis elegans*. *Philos Trans R Soc Lond B Biol Sci*  
621 **314**, 1–340 (1986).
- 622 32. Jarrell, T. A. *et al.* The connectome of a decision-making neural network. *Science* (1979)  
623 **337**, 437–444 (2012).
- 624 33. Zhang, S., Li, F., Zhou, T., Wang, G. & Li, Z. *Caenorhabditis elegans* as a Useful Model  
625 for Studying Aging Mutations. *Front Endocrinol (Lausanne)* **11**, (2020).
- 626 34. Caldwell, K. A., Willicott, C. W. & Caldwell, G. A. Modeling neurodegeneration in  
627 *Caenorhabditis elegans*. *Dis Model Mech* **13**, dmm046110 (2020).
- 628 35. Ding, S. S., Schumacher, L. J., Javer, A. E., Endres, R. G. & Brown, A. E. X. Shared  
629 behavioral mechanisms underlie *C. elegans* aggregation and swarming. *Elife* **8**, e43318  
630 (2019).
- 631 36. Hunt, P. R. The *C. elegans* model in toxicity testing. *J Appl Toxicol* **37**, 50–59 (2017).
- 632 37. Kikin, O., D'Antonio, L. & Bagga, P. S. QGRS Mapper: a web-based server for predicting  
633 G-quadruplexes in nucleotide sequences. *Nucleic Acids Res* **34**, W676–W682 (2006).
- 634 38. Kim, R., Youn, Y.-S., Kang, M. & Kim, E. Platform-and label-free detection of lead ions in  
635 environmental and laboratory samples using G-quadruplex probes by circular dichroism  
636 spectroscopy. *Sci Rep* **10**, 20461 (2020).
- 637 39. Randazzo, A., Spada, G. P. & da Silva, M. W. Circular dichroism of quadruplex structures.  
638 *Quadruplex nucleic acids* 67–86 (2013).
- 639 40. Anderson, G. L., Boyd, W. A. & Williams, P. L. Assessment of sublethal endpoints for  
640 toxicity testing with the nematode *Caenorhabditis elegans*. *Environmental Toxicology and*  
641 *Chemistry: An International Journal* **20**, 833–838 (2001).

- 642 41. Tang, B. *et al.* High-throughput assessment of toxic effects of metal mixtures of  
643 cadmium(Cd), lead(Pb), and manganese(Mn) in nematode *Caenorhabditis elegans*.  
644 *Chemosphere* **234**, 232–241 (2019).
- 645 42. Lu, C., Svoboda, K. R., Lenz, K. A., Pattison, C. & Ma, H. Toxicity interactions between  
646 manganese (Mn) and lead (Pb) or cadmium (Cd) in a model organism the nematode *C.*  
647 *elegans*. *Environmental Science and Pollution Research* **25**, 15378–15389 (2018).
- 648 43. Jomova, K. *et al.* Essential metals in health and disease. *Chem Biol Interact* 110173  
649 (2022).
- 650 44. Lamas, G. A., Ujueta, F. & Navas-Acien, A. Lead and cadmium as cardiovascular risk  
651 factors: the burden of proof has been met. *Journal of the American Heart Association* vol.  
652 10 e018692 Preprint at (2021).
- 653 45. Wang, H. *et al.* Selection and characterization of DNA aptamers for the development of  
654 light-up biosensor to detect Cd (II). *Talanta* **154**, 498–503 (2016).
- 655 46. Wu, Y., Zhan, S., Wang, L. & Zhou, P. Selection of a DNA aptamer for cadmium detection  
656 based on cationic polymer mediated aggregation of gold nanoparticles. *Analyst* **139**,  
657 1550–1561 (2014).
- 658 47. Chute, C. D. *et al.* Co-option of neurotransmitter signaling for inter-organismal  
659 communication in *C. elegans*. *Nat Commun* **10**, 3186 (2019).
- 660 48. Hilliard, M. A., Bergamasco, C., Arbucci, S., Plasterk, R. H. A. & Bazzicalupo, P. Worms  
661 taste bitter: ASH neurons, QUI-1, GPA-3 and ODR-3 mediate quinine avoidance in  
662 *Caenorhabditis elegans*. *EMBO J* **23**, 1101–1111 (2004).
- 663 49. Wang, F., Zuroske, T. & Watts, J. K. RNA therapeutics on the rise. *Nat Rev Drug Discov*  
664 **19**, 441–442 (2020).
- 665 50. Stein, G. S. *et al.* Runx2 control of organization, assembly and activity of the regulatory  
666 machinery for skeletal gene expression. *Oncogene* **23**, 4315–4329 (2004).
- 667 51. Jensen, E. D., Gopalakrishnan, R. & Westendorf, J. J. Regulation of gene expression in  
668 osteoblasts. *Biofactors* **36**, 25–32 (2010).
- 669 52. John, A. A. *et al.* AAV-mediated delivery of osteoblast/osteoclast-regulating miRNAs for  
670 osteoporosis therapy. *Molecular Therapy-Nucleic Acids* **29**, 296–311 (2022).
- 671 53. Hauptman, M., Bruccoleri, R. & Woolf, A. D. An Update on Childhood Lead Poisoning.  
672 *Clin Pediatr Emerg Med* **18**, 181–192 (2017).
- 673 54. Landrigan, P. J., Rauh, V. A. & Galvez, M. P. Environmental justice and the health of  
674 children. *Mt Sinai J Med* **77**, 178–187 (2010).
- 675 55. Waters, R. S., Bryden, N. A., Patterson, K. Y., Veillon, C. & Anderson, R. A. EDTA  
676 chelation effects on urinary losses of cadmium, calcium, chromium, cobalt, copper, lead,  
677 magnesium, and zinc. *Biol Trace Elem Res* **83**, 207–221 (2001).



- 678 56. Davies, N. *et al.* Functionalized lipid nanoparticles for subcutaneous administration of  
679 mRNA to achieve systemic exposures of a therapeutic protein. *Molecular Therapy-*  
680 *Nucleic Acids* **24**, 369–384 (2021).
- 681 57. McDougall, R. *et al.* The Nonclinical Disposition and Pharmacokinetic/Pharmacodynamic  
682 Properties of N-Acetylgalactosamine–Conjugated Small Interfering RNA Are Highly  
683 Predictable and Build Confidence in Translation to Human. *Drug Metabolism and*  
684 *Disposition* **50**, 781–797 (2022).
- 685 58. Ding, D. *et al.* The First-in-Human Whole-Body Dynamic Pharmacokinetics Study of  
686 Aptamer. *Research* **6**, 0126 (2023).
- 687 59. Zhang, Y. *et al.* Impacts of lead exposure and chelation therapy on bone metabolism  
688 during different developmental stages of rats. *Ecotoxicol Environ Saf* **183**, 109441 (2019).
- 689 60. Lamas, G. A. *et al.* Effect of disodium EDTA chelation regimen on cardiovascular events  
690 in patients with previous myocardial infarction: the TACT randomized trial. *JAMA* **309**,  
691 1241–1250 (2013).
- 692 61. Escolar, E. *et al.* The effect of an EDTA-based chelation regimen on patients with  
693 diabetes mellitus and prior myocardial infarction in the Trial to Assess Chelation Therapy  
694 (TACT). *Circ Cardiovasc Qual Outcomes* **7**, 15–24 (2014).
- 695 62. Wang, L. *et al.* Trends in prevalence of diabetes and control of risk factors in diabetes  
696 among US adults, 1999-2018. *JAMA* **326**, 704–716 (2021).
- 697 63. Ahmad, F. B., Cisewski, J. A., Xu, J. & Anderson, R. N. Provisional mortality data—United  
698 States, 2022. *Morbidity and Mortality Weekly Report* **72**, 488 (2023).
- 699 64. Chute, C. D. *et al.* Co-option of neurotransmitter signaling for inter-organismal  
700 communication in *C. elegans*. *Nat Commun* **10**, 3186 (2019).
- 701
- 702